Spectrum Sensing Using Cyclostationary Properties and Application to IEEE 802.22 WRAN

Hou-Shin Chen*† Wen Gao† David G. Daut*
*Dept. of Electrical and Computer Engineering, Rutgers University
94 Brett Road Piscataway, NJ, 08854, USA
†Thomson Corporate Research, Princeton
2 Independence Way, Princeton, NJ, 08540, USA

***Abstract*—Spectrum sensing in a very low SNR environment (less than -20 dB) is considered in this paper. We make use of the noise rejection property of the cyclostationary spectrum. The sensing algorithms are based on measurement of the cyclic spectrum of the received signals. The statistics of the cyclic spectrum of the stationary white Gaussian process are fully analyzed for three measurement methods of the cyclic spectrum. The application to IEEE 802.22 WRAN is presented and the probability of false alarm is analytically derived. The operating characteristic curves for the sensing algorithms are determined from computer simulations using ATSC A/74 DTV signal captures as a test database.**

I. Introduction

Recently, spectrum sensing in an environment with very low signal to noise power ratio (SNR) is becoming an important topic because the operation is an essential function of Cognitive Radio (CR) systems [1]. Under the charter of an IEEE 802 standards committee, a working group named IEEE 802.22 was established to develop a standard for a Cognitive Radio-based PHY/MAC/air_interface for use by license-exempt devices on a non-interfering basis in spectrum that has already been allocated to the TV Broadcast Service. To implement Cognitive Radio without interference to the licensed signal, the sensing tiger team of the IEEE 802.22 group specified the requirements of the spectrum sensing of ATSC DTV signals: the miss detection probability (P_{MD}) should not exceed 0.1 subject to a 0.1 probability of false alarm (P_{FA}) when the SNR is -20.8 dB. In such a low SNR regime, traditional signal detection methods, e.g., power detection, do not work [2]. It is also very difficult for some signature based sensing algorithms to achieve the stated requirements [3]. Spectrum sensing utilizing a signal's cyclostationary property is a possible candidate to achieve the sensing requirements because of its noise rejection ability. It is known that the stationary Gaussian process has a zero-valued cyclic spectrum or spectrum correlation density function (SCD) [4] at nonzero cyclic frequency. Therefore, we can detect the desired signal by computing its cyclic spectrum provided that the signal is cyclostationary such that its cyclic spectrum is not identically zero at some nonzero cyclic frequency. In this paper, we make use of this simple idea to develop a cyclostationarity based spectrum sensing algorithm and apply it to perform spectrum sensing in IEEE 802.22 WRAN.

Ideally, the cyclic spectrum of a stationary random noise process should be zero. However, in practical computation, the cyclic spectrum of a stationary random noise process is a random process. Thus, the samples of the cyclic spectrum are random variables and the detection performance will depend on the behaviors of these random variables. Eventually, in order to be able to detect a signal in a very low SNR environment, we would like to make the variances of these random variables as low as possible. The statistical behavior of the measured cyclic spectrum depends on the measurement method. There are only a limited number of methods in the present literature to measure the cyclic spectrum [5]. Therefore, the development of efficient and accurate algorithms for cyclic spectrum analysis is an important topic of current research.

This paper can be divided into two parts. The first part presents a brief review of cyclostationary properties. Some key equations for cyclostationarity are given in Section II. Then, we will introduce three SCD measurement methods and their digital implementation in Section III, followed by statistical analysis of the SCD of the stationary white Gaussian process. In the second part, we will describe how to apply cyclostationarity to perform spectrum sensing based on its noise rejection ability by measuring the cyclic spectrum of the received signals in Section V. Then, the cyclostationary feature of an ATSC DTV signal is derived and a suitable spectrum sensing algorithm is given in Section VI. The operating characteristic curves for the algorithms developed in this study are determined using computer simulations and are presented in Section VII. The test database consists of ATSC A/74 DTV signal captures obtained from real-word field data. Finally, a conclusion is given in Section VIII.

II. Review of Cyclostationary Properties

In this section, we present a brief summary of some useful equations relevant to cyclostationarity. Details of cyclostationary properties can be found in [4][6]. The cyclic autocorrelation function of a stochastic process $x(t)$ for a given cyclic frequency α can be defined as follows:

$$R_x^{\alpha}(\tau) = \lim_{\Delta t \to \infty} \frac{1}{\Delta t} \int_{-\Delta t/2}^{\Delta t/2} x(t+\tau/2)x^*(t-\tau/2)e^{-j2\pi\alpha t}dt \quad (1)$$

1930-529X/07/$25.00 © 2007 IEEE
This full text paper was peer reviewed at the direction of IEEE Communications Society subject matter experts for publication in the IEEE GLOBECOM 2007 proceedings.

or

$$R_x^\alpha(\tau) = \lim_{\Delta t\to\infty} \frac{1}{\Delta t} \int_{-\Delta t/2}^{\Delta t/2} u(t+\tau/2)v^*(t-\tau/2)dt \quad (2)$$

where $u(t) = x(t)e^{-j\pi\alpha t}$ and $v(t) = x(t)e^{+j\pi\alpha t}$ are frequency shifted versions of $x(t)$ so that $R_x^\alpha(\tau)$ can be understood as the cross-correlation of $u(t)$ and $v(t)$. The cyclic spectrum of $x(t)$ for a given cyclic frequency α is defined as

$$S_x^\alpha(f) = \int_{-\infty}^{\infty} R_x^\alpha(\tau)e^{-j2\pi\alpha\tau}d\tau = S_{uv}(f) \quad (3)$$

where the second equality comes from (2). Thus, the cyclic spectrum $S_x^\alpha(f)$ can also be understood as the cross-spectral density of frequency shifted signals $u(t)$ and $v(t)$. In light of this interpretation, the cyclic spectrum is also called a Spectral Correlation Density (SCD) function. In this paper, we will use the terms cyclic spectrum and SCD interchangeably.

III. Measurement of Spectral Correlation

A. Theoretical Expression

It can be shown that the cyclic spectrum is obtainable from the following limit of *temporally* smoothed products of spectral components described by the expression

$$\begin{aligned} S_x^\alpha(f) &= \lim_{\Delta f\to 0}\lim_{\Delta t\to\infty} \frac{1}{\Delta t}\int_{-\Delta t/2}^{\Delta t/2} \Delta f X_{1/\Delta f}(t, f+\alpha/2) \\ &\quad \cdot X^*_{1/\Delta f}(t, f-\alpha/2)dt \end{aligned} \quad (4)$$

where $X_{1/\Delta f}(t,\nu)$ is the short-term Fourier transform of $x(t)$ with center frequency ν and approximate bandwidth Δf

$$X_{1/\Delta f}(t,\nu) \triangleq \int_{t-1/2\Delta f}^{t+1/2\Delta f} x(\lambda)e^{-j2\pi\nu\lambda}d\lambda. \quad (5)$$

It also can be shown that $S_x^\alpha(f)$ is given by the limit of *spectrally* smoothed products of spectral components

$$\begin{aligned} S_x^\alpha(f) &= \lim_{\Delta f\to 0}\lim_{\Delta t\to\infty} \frac{1}{\Delta f}\int_{f-\Delta f/2}^{f+\Delta f/2} \frac{1}{\Delta t} X_{\Delta t}(t, \nu+\alpha/2) \\ &\quad \cdot X^*_{\Delta t}(t, \nu-\alpha/2)d\nu \end{aligned} \quad (6)$$

where $X_{\Delta t}(t,f)$ is defined by (5) with $1/\Delta f$ being replaced by Δt. Equations (4) and (6) are provided in [5]. We give a third method which is also based on *spectrally* smoothed products of spectral components. Let $x(t,\mu)$ denote the frequency down-converted signal which has carrier frequency μ. Then, the cyclic spectrum is given by

$$\begin{aligned} S_x^\alpha(f) &= \lim_{\Delta f\to 0}\lim_{\Delta t\to\infty} \frac{1}{\Delta f}\int_{f-\frac{\Delta f}{2}}^{f+\frac{\Delta f}{2}} \frac{1}{\Delta t} X_{\Delta t}(t, \mu, f+\alpha/2) \\ &\quad \cdot X^*_{\Delta t}(t, \mu, f-\alpha/2)d\mu \end{aligned} \quad (7)$$

where

$$X_{\Delta t}(t,\mu,\nu) \triangleq \int_{t-\Delta t/2}^{t+\Delta t/2} x(\lambda,\mu)e^{-j2\pi\nu\lambda}d\lambda. \quad (8)$$

Note that (6) and (7) are the same approach for the measurement of spectral correlation. The cyclic spectrum is obtained by *spectrally* smoothed products of spectral components. The difference will be easily seen in their digital implementations.

B. Digital Implementation

The digital implementation of (4), (6) and (7) is based on use of the fast Fourier transform (FFT) algorithm for computation of a discrete-time/discrete-frequency counterpart of the sliding-window complex Fourier transform of (5) and (8). Note that in digital implementation, the frequency variable f and cyclic frequency variable α should be a multiple of F_s. The parameter $F_s = 1/NT_s$ is the frequency sampling increment and T_s is the time-sampling increment. Let $f = lF_s$ and $\alpha = 2DF_s$, the discrete-frequency smoothing method of (6) is given by

$$\begin{aligned} S_x^\alpha[l] &= \frac{1}{(N-1)T_s}\frac{1}{M}\sum_{\nu=-(M-1)/2}^{(M-1)/2} X[l+D+\nu] \\ &\quad \cdot X^*[l-D+\nu] \end{aligned} \quad (9)$$

where

$$X[\nu] = \sum_{k=0}^{N-1} x[k]e^{-j2\pi\nu k/N} \quad (10)$$

which is the DFT of the sampled signal $x[k] = x(kT_s)$, and *M* is the smoothing factor. The parameter *N* is the number of time samples used in DFT. The frequency smoothing method of (7) is given by

$$\begin{aligned} S_x^\alpha[l] &= \frac{1}{(N-1)T_s}\frac{1}{M}\sum_{\mu=-(M-1)/2}^{(M-1)/2} X[l+D,\mu] \\ &\quad \cdot X^*[l-D,\mu] \end{aligned} \quad (11)$$

where

$$X[\nu,\mu] = \sum_{k=0}^{N-1} x[k,\mu]e^{-j2\pi\nu k/N} \quad (12)$$

and $x[k,\mu] = x(kT_s, f_{IF}+\mu\cdot\delta f)$ is frequency down-converted signal having carrier frequency $f_{IF}+\mu\cdot\delta f$. The parameter f_{IF} is an intermediate frequency. Unless otherwise noted, here $x(t)$ is the frequency down-converted signal which has central frequency f_{IF}. Now, we can see the difference of (6) and (7) in their digital implementations. For (6), spectral smoothing is performed over nearby subcarriers of the DFT output given by (10), and therefore, it is called a discrete-frequency smoothing method. As for (7), spectral smoothing is performed over the same subcarrier of the DFT output of down-converted signals which have slightly different carrier frequencies given by (12). Therefore, by controlling the parameter δf, we can obtain more precise frequency resolution without increasing the DFT size. The discrete-time average method is given by

$$S_x^\alpha[l] = \frac{1}{(N-1)T_s}\frac{1}{KM}\sum_{u=0}^{KM-1} X_u[l+D]\cdot X_u^*[l-D] \quad (13)$$

where

$$X_u[\nu] = \sum_{k=0}^{N-1} x_u[k]e^{-j2\pi\nu k/N} \quad (14)$$

which is the DFT of the sliding sampled signal $x_u[k] = x(\frac{u(N-1)T_s}{K} + kT_s)$ The parameter *K* is the block overlapping

1930-529X/07/$25.00 © 2007 IEEE

factor. If *K* is 1, all data segments are non-overlapping. For more details about the measurement of a cyclic spectrum, the reader is referred to [5].

IV. Statistical Analysis of the Measured AWGN SCD

A. Probability Distribution Function of the Computed AWGN SCD Using Equation (9)

Upon substituting $x(t)$ with $w(t)$ which is a white Gaussian process, we will obtain the SCD of an additive white Gaussian noise (AWGN) The corresponding short-term Fourier transform of AWGN is denoted as $W[\nu]$, $W[\nu,\mu]$ and $W_u[\nu]$ in (10), (12) and (14). We know that $w[k]$ are independently and identically distributed (i.i.d.) Gaussian random variables with zero-mean and variance σ^2. It can be easily shown that $W[\nu],\ \nu = 0, 1, \ldots, N-1$ are circularly symmetric i.i.d. complex Gaussian random variables with zero-mean and variance $N\sigma^2$. In (9), the random variable $W[l+D+\nu]W^*[l-D+\nu]$ has zero-mean while its real and imaginary parts are uncorrelated and have the same variance $N^2\sigma^4/2$. Then, by the Central Limit Theorem, for sufficiently large *M*

$$\lim_{M\to\infty} S_w^\alpha[l] \to CN(0, \frac{N^2}{(N-1)^2T_s^2}\frac{\sigma^4}{M}) \tag{15}$$

where $CN(\mu,\sigma^2)$ represents the circularly symmetric complex Gaussian distribution with mean μ and variance σ^2. We can easily determine that the random vectors $\mathbf{S}_w^\alpha = [S_w^\alpha[0], \ldots S_w^\alpha[N-1]]$ are jointly circular symmetric complex Gaussian with zero-mean and possess the covariance matrix

$$Cov(\mathbf{S}_w^\alpha) = E[\mathbf{S}_w^\alpha \mathbf{S}_w^{\alpha\,H}] = \mathbf{T}^S \tag{16}$$

where $\mathbf{T}^S$ is a Toeplitz matrix having the entries

$$T_{mn}^S = \begin{cases} \frac{M-|m-n|}{M^2}\frac{N^2\sigma^4}{(N-1)^2T_s^2} & |m-n| < M \\ 0 & |m-n| \geq M. \end{cases} \tag{17}$$

B. Probability Distribution Function of the Computed AWGN SCD Using Equation (11)

In (11), the random variables $X[l,\mu]$ for different μ are not necessarily independent. However, they are almost independent for sufficiently large difference in frequency index μ or subcarrier index l. Therefore, we assume, for ease of analysis, that they are independent. The resulting distribution yields a good approximation. As a result, it can be easily shown that the distribution of $S_w^\alpha[l]$ is given by (15) for sufficiently large *M*. Furthermore, by appropriately choosing δf, random variables, $S_w^\alpha[l]$'s, are nearly independent.

C. Probability Distribution Function of the Computed AWGN SCD Using Equation (13)

First, we should note that, for the random variables corresponding to the same frequency subcarrier, $W_u[\nu]$ and $W_r[\nu]$ are not independent for $|u-r| < K$ because they are Fourier transformed by overlapping AWGN samples. However, for the random variables taken from different frequency of $W_u[\nu]$ and $W_r[\omega]$ are always independent. Let $Z_u^D[l] = W_u[l+D]W_u^*[l-D]$, note again that the complex random variable $Z_u^D[l]$ has zero-mean, variance $N\sigma^2$, and most important of all, its real part and imaginary part are uncorrelated. Define the random vector $\mathbf{Z}^D[l] = [Z_0^D[l], Z_1^D[l], \ldots, Z_{KM-1}^D[l]]$, then $\mathbf{Z}^D[l]$ is zero-mean with covariance matrix

$$Cov(\mathbf{Z}^D[l]) = E[\mathbf{Z}^D[l]\mathbf{Z}^D[l]^H] = \mathbf{T}^Z \tag{18}$$

where $\mathbf{T}^Z$ is a Toeplitz matrix having the entries

$$T_{mn}^Z = \begin{cases} (1-\frac{|m-n|}{K})^2N^2\sigma^4 e(m,n) & |m-n| < K \\ 0 & |m-n| \geq K \end{cases} \tag{19}$$

where $e(m,n) = e^{-j4\pi D(m-n)/K}$. We can write (13) as

$$S_w^\alpha[l] = \frac{1}{(N-1)T_s}\frac{1}{KM}\sum_{u=0}^{KM-1} Z_u^D[l] \tag{20}$$

and the variance of $S_w^\alpha[l]$ is

$$\begin{aligned} Var(S_w^\alpha[l]) &= \frac{1}{(N-1)^2T_s^2}\frac{1}{(KM)^2}\sum_m\sum_n T_{mn}^Z \\ &= \frac{1}{(KM)^2}\frac{N^2\sigma^4}{(N-1)^2T_s^2} \\ &\cdot(KM + \sum_{i=1}^{K-1}(KM-i)(1-\frac{i}{K})\cdot 2cos(4i\pi D/K)) \end{aligned} \tag{21}$$

Then, by the Central Limit Theorem for the case of dependent random variables,

$$\lim_{KM\to\infty} \frac{S_w^\alpha[l]}{\sqrt{VAR(S_w^\alpha[l])}} \to CN(0,1). \tag{22}$$

Fortunately, the random variables associated with different carriers of $S_w^\alpha[l]$ are independent. Hence, the random vector $\mathbf{S}_w^\alpha = [S_w^\alpha[0], \ldots S_w^\alpha[N-1]]$ obtained by using the discrete-time average method consists of i.i.d. circularly symmetric complex Gaussian random variables having zero-mean and variance given by (21).

D. Discussion

1) Computing SCD by discrete-frequency smoothing method, (9), usually needs a large FFT size which increases overall complexity. We can see from (17) that the random variables of the measured SCD of AWGN noise are dependent. This is an unwanted property and contradictory to the true SCD of AWGN. The inherent dependence of the SCD is also an undesired property in the detection of signal. For example, we may use the maximum of the moving average amplitude of the measured SCD as our decision statistic. The dependence of the random variables of SCD means that large values of the moving average could occur with high probability for AWGN noise. On the other hand, the random variables of the measured SCD of AWGN noise obtained by using the other two methods are independent or nearly independent.

1930-529X/07/$25.00 © 2007 IEEE

2) The variance of the measured SCD of AWGN using discrete-time average method, (13), is given by (21). We can see that if the ratio of *D/K* is $1/2$ or integers, then the *cosine* term becomes 1. As a consequence, the variance of the SCD is approximately the same as the variance of the power spectrum density which means the SCD of AWGN is not approaching zero. This is the cycle leakage effect described in [5] and is revealed here in (21). Therefore, we have to increase the block-overlap parameter *K* to avoid cycle leakage effect. However, increasing *K* results in larger complexity.
3) The computed SCD of AWGN using (11) has the best property that the random variables of different frequency subcarriers are almost independent and there is no cycle leakage effect. However, by using (11) to compute SCD, we have to do down conversion for many times which results large complexity.

In the application of signal detection or spectrum sensing in the presence of AWGN noise, based on the discussion above, we find that the SCD of AWGN measured by three different methods has some drawbacks. The features of cyclic spectrum of the transmitted signal are also different for these three methods. Therefore, we should choose one of the three methods that offers the best tradeoff between needed features and unwanted properties.

V. General Spectrum Sensing System Model

In most communication systems, spectrum sensing is related to the detection of the existence of a specific signal in the presence of AWGN noise. Let $x(t)$ be the transmitted continuous time signal, and it encounters a linear time-invariant channel denoted by $h(t)$. Then, the channel output is corrupted by an AWGN noise $w(t)$. The received signal $y(t)$ is therefore given by

$$y(t) = x(t) \otimes h(t) + w(t) \tag{23}$$

where $w(t)$ is a a white Gaussian process with zero-mean and its cyclic auto-correlation function is given as

$$R_w^\alpha(\tau) = \begin{cases} \sigma^2\delta(\tau), & \alpha = 0 \\ 0, & \alpha \neq 0. \end{cases} \tag{24}$$

In [6], stationary signals are divided into two categories. Those stationary signals with $R_x^\alpha(\tau) \neq 0$ for some $\alpha \neq 0$ are called *cyclostationary* and those stationary signals with $R_x^\alpha(\tau) = 0$ for all $\alpha \neq 0$ are referred to as *purely stationary*. Thus, AWGN is a purely stationary signal. It is shown in [6] that when a signal $x(t)$ undergoes an LTI transformation ($z(t) = x(t) \otimes h(t)$), the input SCD and output SCD are related as

$$S_z^\alpha(f) = H(f + \alpha/2)H^*(f - \alpha/2)S_x^\alpha(f). \tag{25}$$

The function $H(f)$ is the frequency response of the channel impulse response. This relationship can be easily understood by considering the SCD as being the cross-spectrum of the spectral components of $x(t)$ at frequencies $f \pm \alpha/2$ and these two spectral components are scaled by $H(f \pm \alpha/2)$ after passing through an LTI channel. Finally, since in (23) $z(t) = x(t) \otimes h(t)$ and $w(t)$ are independent, the cyclic spectrum of the received signal $y(t)$ is

$$\begin{aligned} S_y^\alpha(f) &= S_z^\alpha(f) + S_w^\alpha(f) \\ &= \begin{cases} S_z(f) + S_w(f) & \alpha = 0 \\ S_z^\alpha(f) & \alpha \neq 0 \end{cases} \end{aligned} \tag{26}$$

and therefore, we have

$$S_y^\alpha(f) = H(f + \alpha/2)H^*(f - \alpha/2)S_x^\alpha(f), \quad \alpha \neq 0. \tag{27}$$

The importance of (26) is that cyclostationary properties provide a way to separate cyclostationary signals from random noise which is purely stationary. As long as the SCD of the received signal is not identically zero, we can perform spectrum sensing by measuring the cyclic spectrum of the received signal.

VI. Application to IEEE 802.22 WRAN

According to [7], ATSC DTV signals are vestigial sideband (VSB) modulated. Before VSB modulation, a constant of 1.25 is added to the 8-level pulse amplitude modulated (8-PAM) signal. Therefore, there is a strong pilot tone on the power spectrum density (PSD) of the ATSC DTV signal. Let $z(t)$ be this pilot tone signal which is a sinusoidal signal in the time domain and further assume that this strong pilot tone is located at frequency f_0 , i.e.,

$$z(t) = \sqrt{2P}\cos(2\pi f_0 t + \theta) \otimes h(t) \tag{28}$$

where *P* and θ are the power and the initial phase of the sinusoidal function respectively. The function $h(t)$ is the channel impulse response. The received signal must contain the signal

$$y(t) = z(t)e^{j2\pi f_\Delta t} + w(t) \tag{29}$$

where $w(t)$ is stationary additive white Gaussian noise and f_Δ is the amount of frequency offset in the unit of Hz. The cyclic spectrum of the received signal must contain the cyclic spectrum of $y(t)$ which is given by (26) and (27) where

$$S_y^\alpha(f) = \frac{P}{2}[\delta(f - f_0 - f_\Delta) + \delta(f + f_0 + f_\Delta)]|H(f)|^2 + \sigma^2 \tag{30}$$

for $\alpha = 0$ and

$$S_y^\alpha(f) = \frac{P}{2}\delta(f)H(f - f_0 - f_\Delta)H^*(f + f_0 + f_\Delta) \tag{31}$$

for $\alpha = \pm 2(f_0 + f_\Delta)$.

A. Cyclostationary Feature Detector

Figure 1 illustrates the overall procedure of the cyclostationary feature detector. Following [8], the capture data is filtered by a 6 MHz bandpass filer and power scaled so that the signal $x[n]$ has preset desired signal power. Then a 6 MHz bandpass noise is added to form the experimental data $y[n]$. Note that the bandpass noise is still purely stationary. Because we would like to detect the pilot tone in the cyclic spectrum, we can filter out those frequency components other than the pilot tone. Therefore, we apply a narrow bandpass filter to obtain a small band which contains the pilot tone and then perform

1930-529X/07/$25.00 © 2007 IEEE
This full text paper was peer reviewed at the direction of IEEE Communications Society subject matter experts for publication in the IEEE GLOBECOM 2007 proceedings.

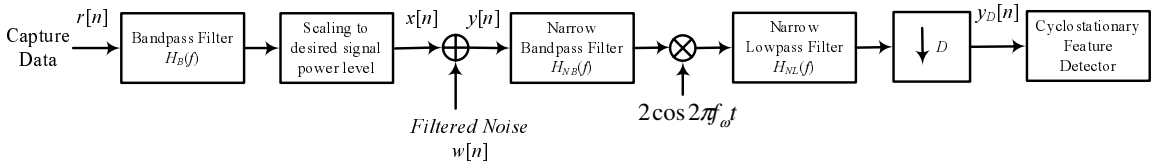

Fig. 1. System implementation of the cyclostationary feature detector.

a D times decimation to reduce the sampling rate in order to reduce the computational complexity. Finally, we compute the cyclostationary feature and make the decision regarding the presence of a signal based on this feature. We will use the frequency average method, (11), to compute the SCD of the received signal because it is the best method to compute SCD which contains pilot tones. According to (31), the pilot tone appears in zero frequency of the cyclic spectrum. Thus, we compute the zero frequency component of cyclic spectra for several cyclic frequencies and use their maximum value as decision statistic

$$T = \max_{\alpha} |S_y^{\alpha}[0]|. \tag{32}$$

B. False Alarm Calculation

Hypothesis H_0 corresponds to the presence of noise only, i.e., $y[n] = w[n]$. The random variables $S_w^{\alpha}[0]$ obtained by using the frequency average method, (11), are nearly i.i.d. circularly symmetric complex Gaussian random variables having zero-mean and variance given by (15). Denote the variance obtained by (15) as σ_S^2, It can be easily shown that the cumulative distribution function of T is given by

$$F_T(t : H_0) = \left(\int_0^t \frac{2u}{\sigma_S^2} e^{-\frac{u^2}{\sigma_S^2}} du \right)^L \tag{33}$$

where L is the number of observed cyclic frequencies. Then, for a particular value of false alarm probability (P_{FA}), the corresponding threshold γ can be found from

$$P_{FA} = 1 - F_T(\gamma : H_0). \tag{34}$$

Finally, after some straightforward calculation, we have

$$\gamma = \rho \left(\sigma_S^2 \ln \frac{1}{1 - (1 - P_{FA})^{1/L}} \right)^{1/2}. \tag{35}$$

where ρ is an heuristic adjusting factor added artificially to account for the approximation mentioned in Section IV-B.

VII. Simulation Results

In Fig. 1, the real-valued DTV signal capture data $r[n]$ are obtained by sampling DTV channels at a rate of 21.524476 MHz, which is 2X over-sampled and then down converted to have a carrier frequency equal to 5.38 MHz [9][10]. Because the pilot tone of the capture data is located around 2.69 MHz. The parameter f_ω in Fig. 1 is (2.69-f_{IF}) MHz. The bandpass filter used to filter the pilot tone has a bandwidth of 40 KHz and f_{IF} is 17 KHz. The decimation factor is 200 and the decimation filter is a 50 KHz low-pass filter. The size of FFT is 2048. The parameter M in (11) is 5 and f_Δ is set to be half of the subcarrier spacing divided by M. The file names of the ATSC DTV signal captures and their corresponding symbols in the simulation figures are listed in Table 1. Figures 2 and 3 show the spectrum sensing performance for $P_{FA} = 0.1$ and $P_{FA} = 0.01$. Both of these simulations use 19.03 ms of sensing time. We can see from Fig's. 2 and 3 that for average detection performance to achieve P_{MD}=0.1, when P_{FA}=0.1, the needed SNR is -25 dB and when P_{FA}=0.01, the needed SNR is -24.3 dB. It means that the proposed algorithm is not sensitive to a change in the P_{FA} (threshold). This is a good feature of the proposed algorithm. Figure 4 shows the spectrum sensing performance for $P_{FA} = 0.1$, and the noise uncertainty equals 1 dB. A 1 dB noise uncertainty means that instead of knowing the exact value of the noise PSD, it has a range of $\pm$ 1 dB. For the discussion of noise uncertainty, interested readers are referred to [11]. We use the worst case scenario, i.e, the PSD of noise is -95.2185 dBm at room temperature, and we assume that the PSD of noise is -94.2185 dBm to calculate the decision threshold. We can see that with 1 dB of noise uncertainty, for average detection performance to achieve P_{MD}=0.1, when P_{FA}=0.1, the needed SNR is -23 dB which reveals that the proposed spectrum sensing algorithm is not sensitive to the noise uncertainty. As for comparison to the other detectors being proposed for IEEE 802.22 WRAN, the best detector in [3] can achieve $P_{MD} = 0.1$ subject to $P_{FA} = 0.1$ when SNR=-13 dB and the sensing time is 90 ms. In [12], the proposed detector can achieve the same performance when SNR=-14 dB and the sensing time is 290.4 ms. Therefore, the proposed detector obviously outperforms the detectors in [3] and [12]. It should be noted that the complexity of the proposed algorithm is relatively less than the detectors proposed in [3] and [12].

VIII. Conclusion

In this paper, we show how to make use of the noise rejection property of the cyclostationary spectrum to perform spectrum sensing in very low SNR environments. The statistical behavior of the estimated cyclic spectrum of a stationary Gaussian process are fully analyzed. The spectrum sensing algorithm for IEEE 802.22 WRAN is developed in detail as well as the calculation of the false alarm rate. The simulation results show that the proposed detector can achieve $P_{MD} = 0.1$ subject to $P_{FA} = 0.1$ when SNR = -25 dB and the sensing time is 19.03 ms. The proposed detector is not sensitive to either changes in P_{FA} or noise uncertainty. Furthermore, the proposed algorithm outperforms the existing signature based sensing algorithms.

1930-529X/07/$25.00 © 2007 IEEE
This full text paper was peer reviewed at the direction of IEEE Communications Society subject matter experts for publication in the IEEE GLOBECOM 2007 proceedings.

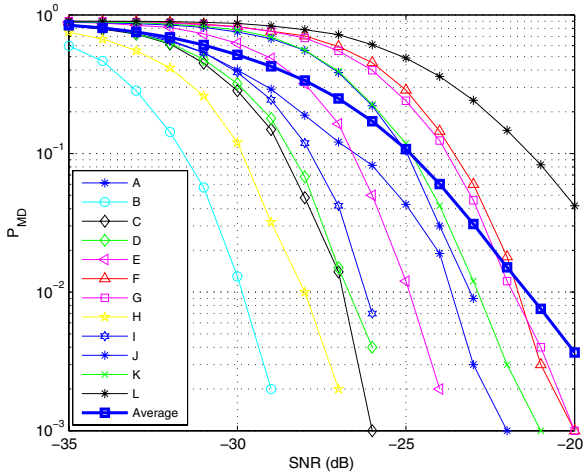

Fig. 2. Spectrum sensing performance of the cyclostationary feature detector, $P_{FA} = 0.1$ and the sensing time=19.03 ms.

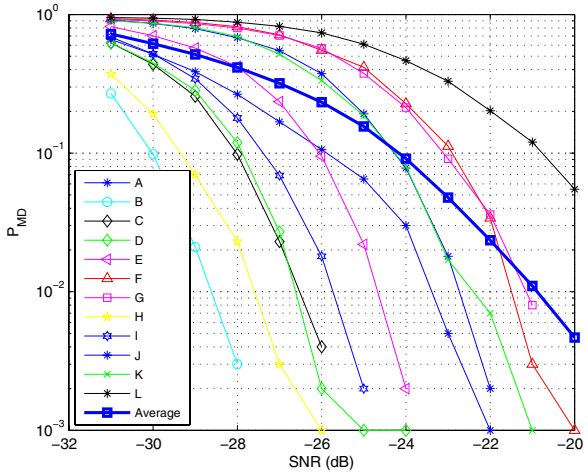

Fig. 3. Spectrum sensing performance of the cyclostationary feature detector, $P_{FA} = 0.01$ and the sensing time=19.03 ms.

Symbol	ATSC DTV Capture Date File Name
A	WAS_3_27_06022000_REF
B	WAS_311_36_06052000_REF
C	WAS_06_34_06092000_REF
D	WAS_311_48_06052000_REF
E	WAS_51_35_05242000_REF
E	WAS_68_36_05232000_REF
F	WAS_86_48_07122000_REF
G	WAS_311_35_06052000_REF
I	WAS_47_48_06132000_opt
J	WAS_32_48_06012000_OPT
K	WAS_49_34_06142000_opt
L	WAS_49_39_06142000_opt
Ave	Average

TABLE I
ATSC DTV CAPTURE DATE FILE NAMES AND ITS CORRESPONDING SYMBOL IN THE FIGURES.

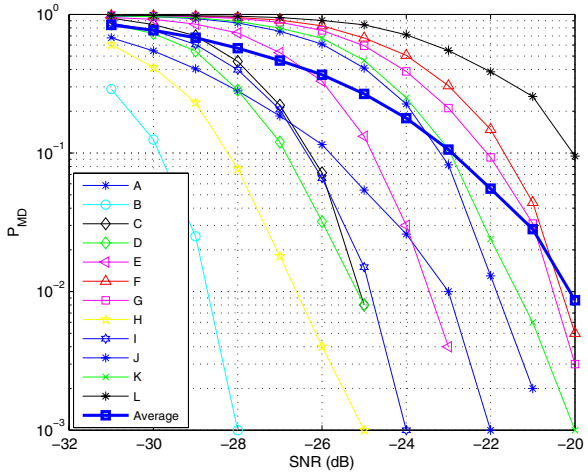

Fig. 4. Spectrum sensing performance of the cyclostationary feature detector, $P_{FA} = 0.1$, noise uncertainty = 1 dB and the sensing time=19.03 ms.

REFERENCES

[1] J. Mitola III, "Cognitive Radio: An Integrated Agent Architecture for Software Defined Radio," Ph.D. Thesis, Royal Institute of Technology, Sweden, May 2000.

[2] S. Shellhammer and R. Tandra, "Performance of the Power Detector with Noise Uncertainty," *IEEE* 802.22-06/0134r0, July 2006.

[3] H. Chen, W. Gao, and D. G. Daut, "Signature Based Spectrum Sensing Algorithms for IEEE 802.22 WRAN," *IEEE* CogNets Workshop (Held in conjunction with *IEEE* ICC 2007), June 2007.

[4] W. A. Gardner, *Statistical Spectral Analysis: A Nonprobabilistic Theory*, Englewood Cliffs, NJ: Prentice-Hall, 1987.

[5] W. A. Gardner, "Measurement of Spectral Correlation," *IEEE Transactions on Acoustics, Speech, and Signal Processing*, Vol. ASSP-34, No. 5, October 1986.

[6] W. A. Gardner, "Exploitation of Spectral Redundancy in Cyclostationary Signals," *IEEE Signal Processing Magazine*, Vol. 8, No. 2, pp. 14-36, April 1991.

[7] ATSC Digital Television Standard, Revision E with Amendments No. 1 and No. 2, ANNEX D, ATSC, Sept. 2006.

[8] S. Mathur, R. Tandra, S. Shellhammer, and M. Ghosh, "Initial Signal Processing of Captured DTV Signals for Evaluation of Detection Algorithms," *IEEE* 802.22-06/0158r4, Sept. 2006.

[9] V. Tawil, "DTV Signal Captures," *IEEE* 802.22-06/0038r0, March 2006.

[10] V. Tawil, "DTV Signal Captures Database," *IEEE* 802.22-06/0081r0, May 2006.

[11] S. Shellhammer and R. Tandra, "Performance of the Power Detector with Noise Uncertainty," *IEEE* 802.22-06/0134r0, July 2006.

[12] S. Shellhammer, "An ATSC Detector Using Peak Combining," *IEEE* 802.22-06/243r5, March 2007.

1930-529X/07/$25.00 © 2007 IEEE
This full text paper was peer reviewed at the direction of IEEE Communications Society subject matter experts for publication in the IEEE GLOBECOM 2007 proceedings.